IN-36

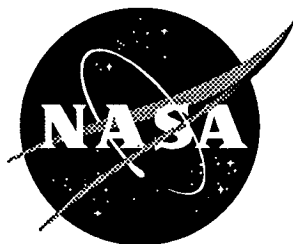*021668*

NASA Contractor Report 201665

Analysis of Particle Image Velocimetry (PIV) Data for Application to Subsonic Jet Noise Studies

James L. Blackshire
ViGYAN, Inc., Hampton, Virginia

National Aeronautics and
Space Administration
Langley Research Center
Hampton, Virginia 23681-0001

Analysis of Particle Image Velocimetry (PIV)
Data for Application to Subsonic Jet Noise Studies

Abstract

Global velocimetry measurements were taken using Particle Image Velocimetry (PIV) in the subsonic flow exiting a 1" circular nozzle in an attempt to better understand the turbulence characteristics of its shear layer regions. This report presents the results of the PIV analysis and data reduction portions of the test and details the processing that was done. Custom data analysis and data validation algorithms were developed and applied to a data ensemble consisting of over 750 PIV 70mm photographs taken in the 0.85 mach flow facility. Results are presented detailing spatial characteristics of the flow including ensemble mean and standard deviation, turbulence intensities and Reynold's stress levels, and 2-point spatial correlations.

Analysis of Particle Image Velocimetry (PIV)
Data for Application to Subsonic Jet Noise Studies

Introduction

Global velocimetry measurements were recently taken as part of the Advanced Subsonic Technology (AST) program at NASA Langley Research Center. In these measurements, Particle Image Velocimetry (PIV) was used to measure the flow exiting a heated 1-inch circularly-symmetric subsonic jet. The PIV technique provided spatially resolved velocity measurements in the shear region of the expanding jet that were used to study turbulence and length scale interaction, and their involvement in the jet-noise production process. Data was taken along a plane intercepting the jet centerline, and included instantaneous, fluctuating, and ensemble mean velocity, as well as ensemble standard deviation levels, turbulence intensities, Reynold's stress, and 2-point correlations.

The specific goal of this effort was to test the feasibility of making in-situ global velocity measurements with the PIV technique in the very harsh environment of a subsonic/transonic jet combustor where temperatures are typically in excess of 500 degrees Farenheit, velocities range from near zero in the entrainment regions to 1.2 mach in the jet core, and vibration and image degradation levels can be severe. Consequently, the PIV analysis processing for this test involved not only evaluation of the basic flow parameters, but determination of image quality levels, measurement accuracy estimates, and data convergence evaluations.

Particle Image Velocimetry (PIV) System Description

The basic PIV measurement process involves taking an instantaneous, double exposure record of seed particles entrained in a flow of interest.[1] Two overlapping laser light sheets are used to illuminate a measurement plane in the flow which has been seeded with neutrally buoyant particles. Digital or photographic records of the tracer seed are then taken, where a delay is introduced between the two laser pulses to allow the particles to move within the exposure. The local velocity, u, can then be determined from the particle image displacement measurements in the film recording using[2]:

$$u = \frac{\Delta X}{\Delta \tau\, M} \tag{1}$$

where ΔX is the local measured particle displacement, $\Delta \tau$ is the laser pulse separation time, and M is the system magnification.

The PIV acquisition system used in this effort is depicted in Figure 1. It uses two frequency doubled Nd:YAG lasers each operating at a wavelength of 532nm, energy of 580mj, and 10Hz repetition rates. A 70mm Hassalblad camera system using Kodak Tri-X film was used

to photograph the flow. The camera used a 350mm focal length lens system operating at F#11, which provided a system magnification of 1:1 and a useable field of view of approximately 55mm^2 (Figure 2). A custom polarizing image shift cube system was placed just before the lens system to resolve directional ambiguity and increase dynamic range levels. The entire imaging system was placed in a sealed enclosure box that was cooled with air conditioned air. This isolated the lens and camera system from the 580 degree F air that was exiting the jet, while allowing it to be within approximately 1/2 meter from the flow. Seed to the jet was provided through one internal and two external seed insertion systems. The external systems were placed along the outer jet structure approximately 12" before the nozzle exit, while the internal system was coupled to the interior of the jet approximately 1 1/2 meters upstream. The internal system was also heated to match the heated air entering the back of the jet.

PIV Analysis Process

The analysis system used in this test is based on a typical PIV analysis system design and uses autocorrelation processing of 8-bit digitized 128x128 pixel sub-regions of a double exposure PIV photograph. In a double-pulsed, single-frame PIV system, the spatial autocorrelation of *I(X)*, the transmitted light intensity from the photograph, with particle image separation levels *s* is approximated by the spatial average estimator over an interrogation spot[3]:

$$R(s) = \int I(X)I(X+s)dX \qquad (2)$$

which consists of five components:

$$R(s) = R_c(s) + R_p(s) + R_{D^+}(s) + R_{D^-}(s) + R_F(s), \qquad (3)$$

Here, R_c is the convolution of the mean intensities and R_F is the fluctuating noise component of the correlation estimator. They represent noise and background influences to the signal levels and are minimized if possible. The signals of interest are given by the $R_D^+(s)$ and $R_D^-(s)$ terms. $R_D^+(s)$, the correlation of all first images shifted by *s* with subsequent unshifted images, and $R_D^-(s)$, the correlation of all later images shifted *s* with prior unshifted images, are identical in form and shape, with $R_D^+(s)$ centered at the <u>positive mean displacement</u> of the images and $R_D^-(s)$ centered at the <u>negative mean displacement</u>. The strongest signal component R_P, represents the correlation of particle images with themselves, and has a maximum value when s=0 and a width comparable to dτ, the particle image diameter. The amplitudes of R_D^+ and R_D^- are less than half that of R_P as the correlation between pairs of images is at most half of the correlation of images with themselves.

The computation intensive 2-D spatial autocorrelation calculations were performed in this effort using an Alacron i860 array processor subsystem on an 486/33 IBM PC/AT host computer.

The system is currently capable of processing five displacement vectors per second. Custom processing and control software is used and runs under Microsoft Windows v3.1 and Windows 95. The analysis is completely automated with the exception of user input to a configuration file prior to analysis execution for update of various system parameters. The executable program file is named **PIV54.exe** with a configuration text file called **KODAK54.cfg**.

The main system components used in the analysis system include a Kodak Megaplus camera model 1.4, an Epix 4MEG VIDEO Model 10 frame grabber board, an Alacron AL860XP array processor board, and a *Unidex 11* 3-axis motion control system. In addition, a single 120mm focal length, 40mm diameter, achromatic lens imaged the approximate 6mm x 4mm field of view @ 1:1 imaging to the Kodak camera system. A schematic diagram of the system design is provided in Figure 3. The Kodak Megaplus camera has two primary operating modes: low resolution and high resolution. The low resolution mode was used for this set of tests which provided image capture at 640x480 pixel resolution. The image was transferred by the Epix framegrabber board to PC-AT memory and then to the Alacron array processor memory for autocorrelation processing.

A preliminary analysis system checkout was performed before actual analysis began in order to determine the acquisition and analysis magnification levels, spatial resolution levels, and image distortion levels. The acquisition system magnification of 0.93066x was determined by taking several photographs of a 70mm x 70mm grid (@ 1mm grid spacing) with the PIV acquisition system. These raw grids were then examined with the analysis system, and a comparison was made between the photographs and the raw grid in order to calibrate the acquisition system magnification. Five horizontal and six vertical strips of grid data were extracted across the entire field for both the photograph and the raw grid, where measurements of the grid line separations were made and compared.

The analysis system magnification of 10.0628 microns/pixel was found by examining a precision reticle (1mm long @ 50 micron line resolution) at five position covering the entire field of view. The average positions of 20 lines separated by 50 microns each was measured at each location in the vertical and horizontal directions, where the average of the five locations was used to obtain the overall analysis system magnification.

An approximate 1mm spatial resolution was desired (1mm x 1mm correlation cell size) at 50% oversampling which would have given a step size of 0.5mm. The field coverage for a typical PIV photograph taken with the 70mm Hasselblad camera has an octagon shape covering and approximate 55mm x 55mm region at 1:1 magnification (see Figure 2). The analysis system magnification factor of 10.0628 microns/pixel was used with the fact that correlations are done at a 128x128 digitized pixel resolution to obtain a spatial correlation resolution size of: $128pixel^2 *$ 10.0628micron/pixel = 1.2880 mm^2. At 50% over-sampling the vector output resolution is 1/2 the correlation resolution and is 0.644mm (close to the desired 0.5mm resolution) in both the

4

vertical and horizontal directions. The Kodak Megaplus 1.4 camera was used in low resolution mode and captured 640x480 pixels at a time. This allowed a 6x9 grid (50% oversampled) of 128x128 pixels to be captured at a time giving 54 correlations (i.e. vectors) every time the Megaplus camera captured an image. The corresponding step sizes are then (6 x 1.288mm) = 3.864mm in the vertical direction and (9 x 1.288mm) = 5.796mm in the horizontal direction. For an approximate field coverage of 55mm x 55mm, the required number of steps becomes: (55mm / 3.864mm) = ~15 steps in the vertical direction and (55mm / 5.796mm) = ~10 steps in the horizontal direction. And so, the important numbers used in the analysis configuration/setup were:

Spatial resolution of step size:	0.644mm
Step size and step number vertical:	3.864mm @ 15 steps
Step size and step number horizontal:	5.796mm @ 10 steps

The spatial coverage was (15 x 6 x 0.644mm) = (10 x 9 x 0.644mm) = 57.3161mm^2, with (10horiz.steps x 9vectors) = 90 vectors, (15vert.steps x 6vectors) = 90 vectors. This gives 90x90 = 8100 vectors per file/film frame.

A basic image distortion check of the PIV PC/AT analysis system was also performed the results are presented in Figure 4. A computer generated PIV image was used to check the imaging/correlation process across the field of view (FOV) of the Kodak Megaplus 1.4 camera system in low resolution mode. The imaging system currently in use uses a single 120mm achromatic lens to image the PIV photographic field to the 640x480 pixel Megaplus camera field.

The process used to check the distortion present in the imaging system involved correlating the computer generated PIV particle pair field at various positions along the imaging field of view, and measuring correlation peak centroid variations. In order to make sure each portion of the field had the same image field to correlate, the Unidex motion control system was used to move the correlating image field to each distortion check position until the entire field was covered. In total, a 6x9 grid was covered at 50% oversampling (the same grid/oversampling parameters used in a normal analysis). The results show distortion levels of less than 1% with a standard error of approximately 0.41%. The distortion pattern could not be characterized as ‿ pincushion or barrel in nature, but rather had a top-to-bottom tilt structure. This is most likely due to minor deviations in the relative orientation of the object/lens/image planes, which should be perfectly parallel to each other. The errors being introduced to the data by this analysis system distortion are minimal, however, and are within/below the acceptable 1-5% PIV accuracy levels.

The basic analysis process included three steps. First, the film was loaded into the analysis system, where it was aligned so that the horizontal and vertical film positions were lined up with the Unidex motion directions. The film was then moved so that the registration point (a star pattern on the right corner of the nozzle output) was properly aligned. This is depicted in Figure 5. The film

was finally moved to the 0,0 analysis position by moving -45mm in the horizontal direction and +15mm in the vertical direction.

The next step involved setting up the configuration file which is described in more detail below. Once the configuration file was properly setup, the analysis system program was run. This process started an automated autocorrelation analysis routine that moved the film in a stepwise manner 10 positions in the horizontal direction (5.796mm each step), and 15 positions in the vertical direction (3.864mm each step). A low resolution (640x480) Kodak Megaplus image was captured at each position where 50% oversampling provided a 9x6 vector field @ a 128x128 pixel resolution (i.e. correlation) size. The output vector field included an ASCII listing of 11 float numbers representing the horizontal and vertical position of the vector, and the centroid positions and peak values for the top three centroid positions in the search box region.

The autocorrelation algorithm used in this set of tests was originally developed in 1993 with two minor upgrades/revisions occurring in 1994 and 1995, respectively. The processing involves eight sequential steps and include: 1) image thresholding, 2) default image pair inclusion, 3) autocorrelation calculation, 4) zero out DC peak, 5) apply search box restriction, 6) apply centroid threshold, 7) compute centroids, and 8) write data to file.

Step 1 involves thresholding the raw image according to a weighted mean of the image intensity level, where the weighting value is provided by the user in the configuration file. The values used in this test varied between 0.9 and 1.05, where raw image values above the product of the average image intensity and the weighting value were set to 255 (the maximum background image value where the PIV images are recorded as black dots on a white background). A set of three very-weak intensity particle images were then included in step 2 in the raw image data array for discerning saturated or totally black image regions on the frame. This step was included to allow void, non-seeded, and obstructed regions of the frame to be easily deleted in the validation process and has no impact on regions with adequate seeding levels present. A standard autocorrelation processing step was then applied to the data in step 3. The autocorrelation DC peak was then zeroed out of the correlation image in step 4 given the user's configuration value for its extent. These values typically ranged from 4-12 pixels extending radially out from the center of the image. Step 5 involved the application of a restricted search box region given user configuration input values for its positioning and extent. Careful consideration and testing was provided in this step to ensure 1) that the box was properly placed, and 2) that its extents allowed for dynamic movement of the particle positions across the entire field of view. Typical search box extents ranged from +/-25 pixels in the axial direction and +/-15 pixels in the transverse direction, which corresponds to velocity dynamic ranges of +600m/s to -200m/s in the axial direction and +/-200m/s in the transverse direction. Step 6 involved application of a user defined centroid threshold level where values below the designated level were set to zero. This level was typically

6

240 (out of a maximum level of 255). In step 7, a weighted mean centoid computation was then applied to all the remaining correlation peaks in the search box, where correlation patterns with areas > 100 pixels were discarded, and the top three weighted mean centroids were written to file in step 8.

An example configuration file input is provided below. It provides information related to the output file name(s), Kodak Megaplus setup parameters, image thresholding levels, etc.

software_version_number	1.2
exposure_level(ms)	90
#steps_xdimension	10
#steps_ydimension	15
output_timefile_name	time54.dat
image_threshold_level(0-255)	1.0
FP_DC_peak_extent(1-20)	10
search_box_xmin(0-128)	35
search_box_xmax(0-128)	79
search_box_ymin(0-128)	10
search_box_ymax(0-128)	39
Default_peak_xpos(0-64)	0
Default_peak_ypos(0-64)	38
Centroid_threshold_level(0-255)	250
pixel_scale_factor(microns/pixel)	10.0628
acquisition_magnification	0.93066
laser_pulse_separation(microsec)	0.60000
unidex_xshift_amount(microns)	5796
unidex_yshift_amount(microns)	-3864
output_datafile_name	f71r7.dat

PIV analysis system configuration file: **KODAK54.CFG**

The input configuration file supplied various analysis system parameters needed for processing. The system checkout process provided six parameters including the acquisition and analysis magnification factors, the Unidex shift amounts in the x and y directions, and the number of steps in each direction. The initial setup of each roll of film provided ten additional analysis parameters. The exposure level of the Kodak Megaplus camera (in milliseconds) was determined first, where test correlations were used at various exposure levels to optimize the exposure level for a typical frame on a given roll. Image and centroid threshold levels were also evaluated with respect to test correlations at this time. The image threshold factor applies a threshold to the raw image before FFT processing based on the average pixel intensity in the image. The centroid threshold level limits the centroid search to pixel intensity values above a certain level. The DC peak pixels are also zeroed out based on an evaluation of their radial extent out from the correlation image center. Correlation search box limits are then set allowing for movement of the

correlation peak at various positions across the field. And finally, a default peak correlation position is inserted in the event of a totally black or totally white image field.

PIV Data Validation

Following the analysis of all the PIV film frames, a semi-automated PIV vector validation process was performed. These data validation efforts involved two different types of validation processes - individual roll validation and ensemble validation. The individual roll validation processing was done first, and involved several different types of validator algorithms. Two additional ensemble validation steps were then applied to the data that took into account the ensemble mean and standard deviation level at each point in the flow.

The individual roll validation involved 5 steps for the image-shift calibration frames, and 4 steps for the actual data frames. Both the calibration and data files included a bandpass validator, a local median validator, and a 3x3 mean filter processor. An additional ensemble average and manual vector validator step was then applied to the calibration files, while an additional image-shift removal step was applied to the data files. The vector plots in Figure 6 provide a step-by-step example of the results of each validation step from a raw data file input to the final validated file output.

The bandpass validator was applied first, and was used to remove vectors that were obviously bad. A set of high and low threshold levels were chosen for both the u and v components, and if a vector was outside of these high/low threshold ranges, it was zeroed out. Unfortunately, this step required a considerable amount of user input and judgment, and because of this, very liberal limits were chosen for each roll of film. The executable validation program for this step was **HILO.EXE** with the threshold levels being provided by the configuration file **VALIDATE.CFG**.

A local median validator was then applied to the data. In this processing step, a given vector position was compared with the median value of its 8 nearest neighbors. If the absolute value of the difference between the local median and the vector was greater than three times the standard deviation of the 8 nearest neighbors, it was zeroed out. No user input was required for this step. The executable validation program for this step was **LOCMED.EXE**.

A 3x3 mean filter operation was then applied to the data, which involved evaluating the mean of a vector position and its eight nearest neighbors and replacing that vector position with the mean. This step provided a limited amount of smoothing and interpolation to the data, and like the median validator, required no user input. The executable for this step was **3X3MEAN.EXE**.

An ensemble average program was then applied to each roll's image-shift calibration file to obtain an average image shift file for that roll. The executable program for this step was **ENSEMBLE.EXE**, with file name inputs being provided by the file **VALADD.CFG**.

A final manual vector extraction validation step was applied to each ensemble averaged calibration file to remove obvious outlying vectors. The resulting calibration files were then subtracted from each data file in an image shift bias removal step. The executable program for this step was **UNSHIFT.EXE**, with file name inputs being provided by **VALIDATE.CFG**.

Following the individual roll validation, an ensemble bandpass validator was applied to all the data files, which removed vectors outside a given u and v range relative to a preliminary ensemble mean value at each point. The determination of the threshold u and v ranges required user input, and were ultimately chosen to be +/-125m/s for u and +/-75m/s for v. The final ensemble mean validator compared a given vector position to a new preliminary ensemble mean value, and if the absolute value of the difference between the ensemble median and the vector was greater than three times the ensemble standard deviation, it was zeroed out. The executable programs for these two steps were **ENS_HILO.EXE** and **ENS_MEAN.EXE**, respectively.

Like the PIV analysis program, the various validation algorithms required the input of configuration text files for validation parameter setup. The individual roll validators used a text file named **VALIDATE.CFG**, and the ensemble validator used a text file named **VALADD.CFG** for file name input/output. An example individual roll configuration input file is provided below:

```
software_version_number            1.1
Use_Local_Mean_Validator_(y/n)?    y
Use_Local_Median_Validator_(y/n)?  y
Use_Global_Mean/SD_Validator_(y/n)? y
Upper_Threshold_Level_for_U:       -9.5
Lower_Threshold_Level_for_U:       -34.0
Upper_Threshold_Level_for_V:       50.0
Lower_Threshold_Level_for_V:       41.0
Number_of_Vectors_in_x_direction:  90
Number_of_Vectors_in_y_direction:  90
Default_peak_Amount_in_x_direction: -0.0001
Default_peak_Amount_in_y_direction: 20.000
Input_File_Name                    f90r9.v4n
Output_Vector_File_Name            f90r9.v4t
Output_Stats_File_Name             Stats.dat
Input_Calibration_File_Name        r9add46.v6
Standard_deviation_Multiplier:     3.0
```

PIV validation configuration file: **VALIDATE.CFG**

The validation configuration file supplied three basic parameters for the validator algorithms. Upper and lower bounds were provided for the u and v components in the bandpass validator algorithm, a multiplier was provided for the standard deviation amount in the local median validator, and file input/output names were finally provided.

A final part of the data validation processing involved determining vector validation rates (the percentage of actual good vectors extracted from the data relative to the maximum possible that could be extracted). As previously mentioned, a 90x90 vector grid was analyzed for each frame of film, which gives a total possible vector number of 8100 vectors per file. Because the analysis grid setup (see Figure 2) was slightly bigger than the octagonal frame exposure, the maximum vector number was actually limited to only 6935. The plot presented in Figure 7 reflects this maximum vector rate, where a 100% vector rate indicates all possible analyzed positions produced a validated vector (6935 total vectors). Validation rates ranged from ~10-70% per file, with the majority of files falling between 40-50%, and an overall vector rate of approximately 45%.

Results

As previously mentioned, an evaluation of image and autocorrelation signal qualities was performed as part of this test. An initial set of low speed/cold flow PIV photographs produced images of good to excellent quality across the entire field of view. The introduction of heat and increased flow speeds tended to degrade the image quality, however. Some of these effects are depicted in Figure 8. In particular, a blurring of the particle images was noticed just past the nozzle exit, a lack of image pairs was notices in certain regions of the field, and image 'quads' were recorded in certain regions of the downstream flow. These were most likely due to thermal gradient, light sheet overlap, and light sheet polarization problems, respectively. The image blurring near the nozzle exit was noticed on all of the hot/high speed flow photographs and was consistent in its position, coverage, and effect. A lack of image pairs was noticed in approximately 1/2 of the hot/high speed photographs and 1/4 of the cold/low speed photos, and tended to be present downstream of the nozzle. Image quads were present in about 1/2 of the hot/high speed photographs and tended to be sporadically placed downstream in the main jet core. Examples of the auto-correlation patterns produced by these various particle image qualities are provided in Figure 9. The images with quads produced multiple correlation peaks, the blurred images produced correlations with increased size and lowered SNRs, and the images with no pairs produced uncorrelated results.

A total of 417 data files were available for ensemble and turbulence statistics calculations. Plots depicting the ensemble mean vector field are provided in Figures 10-15. Transverse and axial vector component contour plots are provided in two of the plots, as well as a contour plot of the number of vectors available for the ensemble at each field point. The executable program used in this processing step was **ENSEMBLE.EXE**, with filename inputs being provided by the configuration file **VALADD.CFG**.

The ensemble average velocity at each point was then subtracted away from the instantaneous velocity in each file to produce a fluctuating velocity at that point. The involved applying the executable program **FLUCT.EXE** to each validated data file to produce a new fluctuating velocity file with the new extension ***.flc**. An example of the fluctuation velocity output vector field is presented in Figure 16.

Several turbulence statistics calculations were then calculated using the fluctuating velocity files, the results of which are presented in Figures 17-19. They include plots of axial and transverse turbulence intensity levels $<u'u'>$ and $<v'v'>$, Reynold's stress $<u'v'>$, and the number of vectors used in the ensemble for each point in the field. The executable program for this processing was named **TURBSTAT.EXE**.

Two data convergence tests were also applied to the ensemble averaged data. These included convergence of the ensemble axial velocity mean and convergence of the turbulence intensity $<u'u'>$. Data convergence was determined for flow points in the 1) entrainment region, 2) the shear region, and 3) the jet core region. Results are presented in Figures 20 and 21.

Because the data was taken from a plane through the jet axis centerline, and because of the nature of the circular nozzle configuration, the flow exiting the jet was nearly symmetric about the jet axis. This allowed the ensemble average of the data to be increased by folding the data about the jet axis. Results for this increased data ensemble are provided in Figures 22 thru 26. In an attempt to increase the maximum number of data points available for the final ensemble average, a slightly different validated data set was used for the symmetric folded data set ensemble. This validated data set excluded the final ensemble mean validation step, thus concluding with the ensemble bandpass validation step. By doing this, the maximum ensemble number was increased to over 580 in some locations (versus only ~350 available for the ensemble mean validation step). An additional set of fluctuating velocity files were computed based on this alternate ensemble average file, which were used to calculate turbulence statistics data. An additional data convergence test also was performed for the ensemble mean of this new data set and is provided in Figure 27.

Some fluctuations of the image shift bias being introduced into the data were also noticed from film roll to roll, and film frame to frame, which could have an effect on data quality. A study of the amount of fluctuations present, and their effect on the data was consequently done the results of which are presented in Figures 28 thru 30 and Table 1. The Frame-to-Frame variation is depicted in Figure 28 for film Roll #9 which had 15 calibration shots to work with. The axial and transverse image shift values are shown for 9 positions (see Figure 30 for the relative position locations) and showed a positive linear relationship as the frame number increased. An approximate 1.5m/s increase was noticed from frame to frame. A study of the variation of image shift across the field of view using the same 9 points (Figure 29) indicated absolute variations ranging from +5 m/s increase in the lower left corner position for the transverse component, to +

28 m/s for the left axial component position. No real patterns could be discerned. Roll-to-Roll variations are shown in Table 1 where the average standard deviation of each roll was computed. These standard deviation values ranged from 4.88m/s-25.9m/s for the axial component and 4.01m/s to 16.14m/s for the transverse component. Average standard deviations of 13.48m/s and 8.51m/s were computed from these values, respectively. This gives an average standard deviation magnitude of : sqrt($13.48^2 + 8.51^2$) = 15.94m/s, which gives an indication of the errors being introduced by the image shift, in that the ensemble mean of these calibration frames were used for data reduction, and deviations away from this mean were also present in the data sets. This provides an error estimate due to the image shift variations of 15.94/385 = 4.14% relative to the maximum velocity range of 385m/s in the flow.

Because vector validation rates were only 40-50%, a gaussian filter/interpolation algorithm was developed and applied to the available 417 data files. The algorithm applies a gaussian weighting function for positions in the vector field that do not have vectors present, and uses the 10 nearest neighbors for interpolation. The gaussian weighting gives vector positions close to the center position strong weighting in the interpolation process and positions further away less and less weighting according to a gaussian profile. Vector positions that have valid vectors are not subjected to the interpolation/filtering operation and are left unchanged. The program took the final validated data set (*.fin) as input and output the results in files with the extension *.gfn. A new set of fluctuating velocity files was evaluated using these new interpolated files and were given the file extensions *.gfl. An example of the gaussian interpolator is presented in Figure 31 where the original *.fin file is shown at the top of the figure and the gaussian filter/interpolator output is shown on the bottom.

A 2-point correlator algorithm was finally developed and applied to the gaussian interpolated fluctuating velocity files for several positions in the shear region of the flow. The algorithm calculates 5 NxN matrices according to $<u'_i u'_j>$, $<u'_i v'_j>$, $<v'_i u'_j>$, $<v'_i v'_j>$, and $<ij>$, where i and j go from 0 --> N, u' and v' represent the fluctuating velocities at neighboring positions in the flow, and < > represents the ensemble averaging process. The algorithm takes the input from a configuration file named **2PTCOR.CFG**, and has an executable file name of **2PT_COR.EXE**. The 2-point correlations were calculated for a position in the upper shear region of the flow corresponding to 12.88mm above the jet centerline and 5.15mm downstream of the nozzle. Results are presented in Figure 32.

Summary

Over 750 70mm PIV photos were analyzed in the subsonic flow exiting a 1" circular nozzle in an attempt to better understand the turbulence characteristics of its shear layer regions. Custom data analysis and data validation algorithms were developed and applied to a data

ensemble. Results are presented detailing spatial characteristics of the flow including ensemble mean and standard deviation, turbulence intensities and Reynold's stress levels, and 2-point spatial correlations.

Acknowledgements

The author wishes to thank W.M. Humphreys and S.M. Bartram of the Measurement Science and Technology Branch for providing the PIV 70mm photographs, and for assistance and guidance in development of the various algorithms used in this effort. Thanks are also extended to Dr. J. Seiner of the Aero Acoustics Branch, and Dr. M. Glauser of Clarkson University for their guidance and assistance with the nozzle, flow characteristics, and development of turbulent statistics software.

References

[1] Adriane, R. J., "Scattering Particle Characteristics and Their Effect on Pulsed Laser Measurements of Fluid Flow: Speckle Velocimetry vs Particle Image Velocimetry," Appl. Opt. 23, 1690 (1984).

[2] Liu, Z., Landreth, C.C., Adriane, R.J., and Hanratty, T.J., "High Resolution Measurements of Turbulent Structure in a Channel with Particle Image Velocimetry," Exp. Fluids, 10, 1991, 301-312.

[3] Keane, R.D., and Adriane, R.J., "Theory and Simulation of Particle Image Velocimetry," SPIE Vol. 2052 Laser Anemometry Advances and Applications, (1993), p477.

[4] Yao, C., and Paschal K., "PIV Measurements of Airfoil Wake-Flow Turbulence Statistics and Turbulent Structures," 32nd Aerospace Sciences Meeting and Exhibit, Reno, NV, January 10-13, 1994.

[5] Humphreys, W.M., Bartram, S.M., and Blackshire, J.L., "A Survey of Particle Image Velocimetry Applications in Langley Aerospace Facilities," *31st Aerospace Sciences Meeting & Exhibit*, AIAA 93-0411, Reno, NV, January 11-14, 1993.
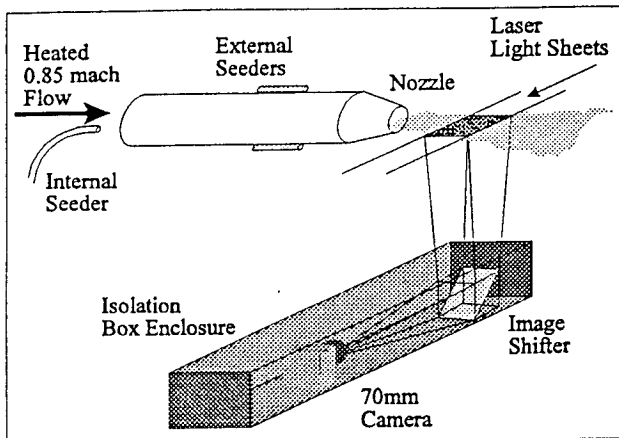
Figure 1. Particle Image Velocimetry acquisition system.

Approximate Film Coverage at 1:1 Magnification
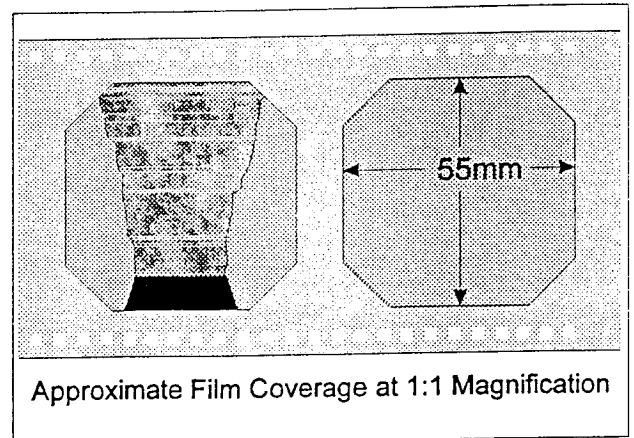
Figure 2. Image Field of View coverage.
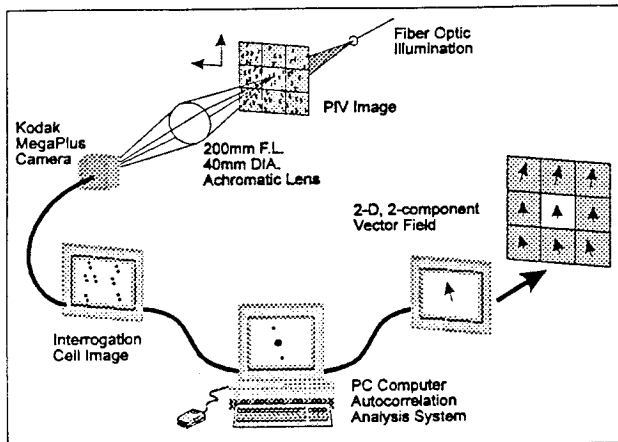
Figure 3. PIV PC/AT Analysis system.

Distortion % for PC/AT Analysis System

(Kodak Megaplus 1.4 in low res mode and 120mm achromatic lens at 1:1 magnification)
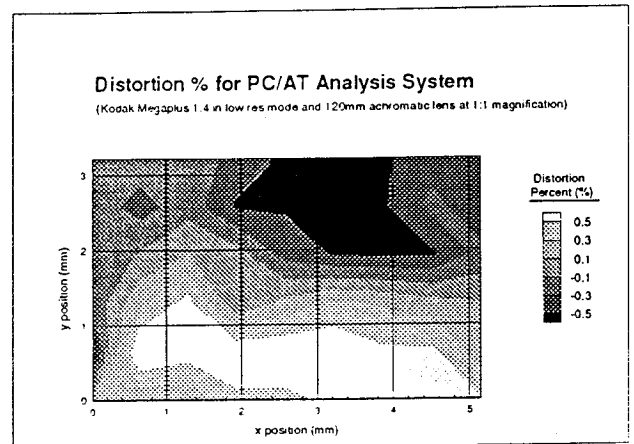
Figure 4. Analysis system image distortion results.

Analysis Grid Setup
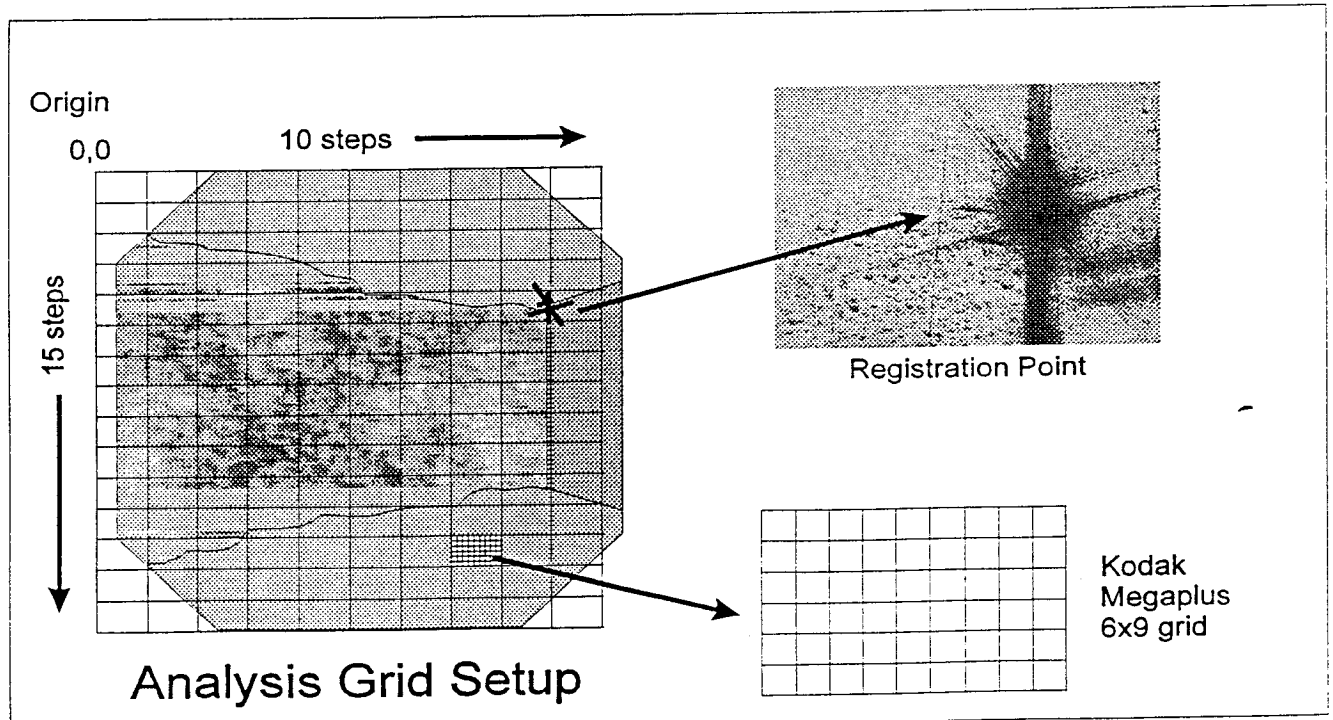
Figure 5. Image registration and setup.
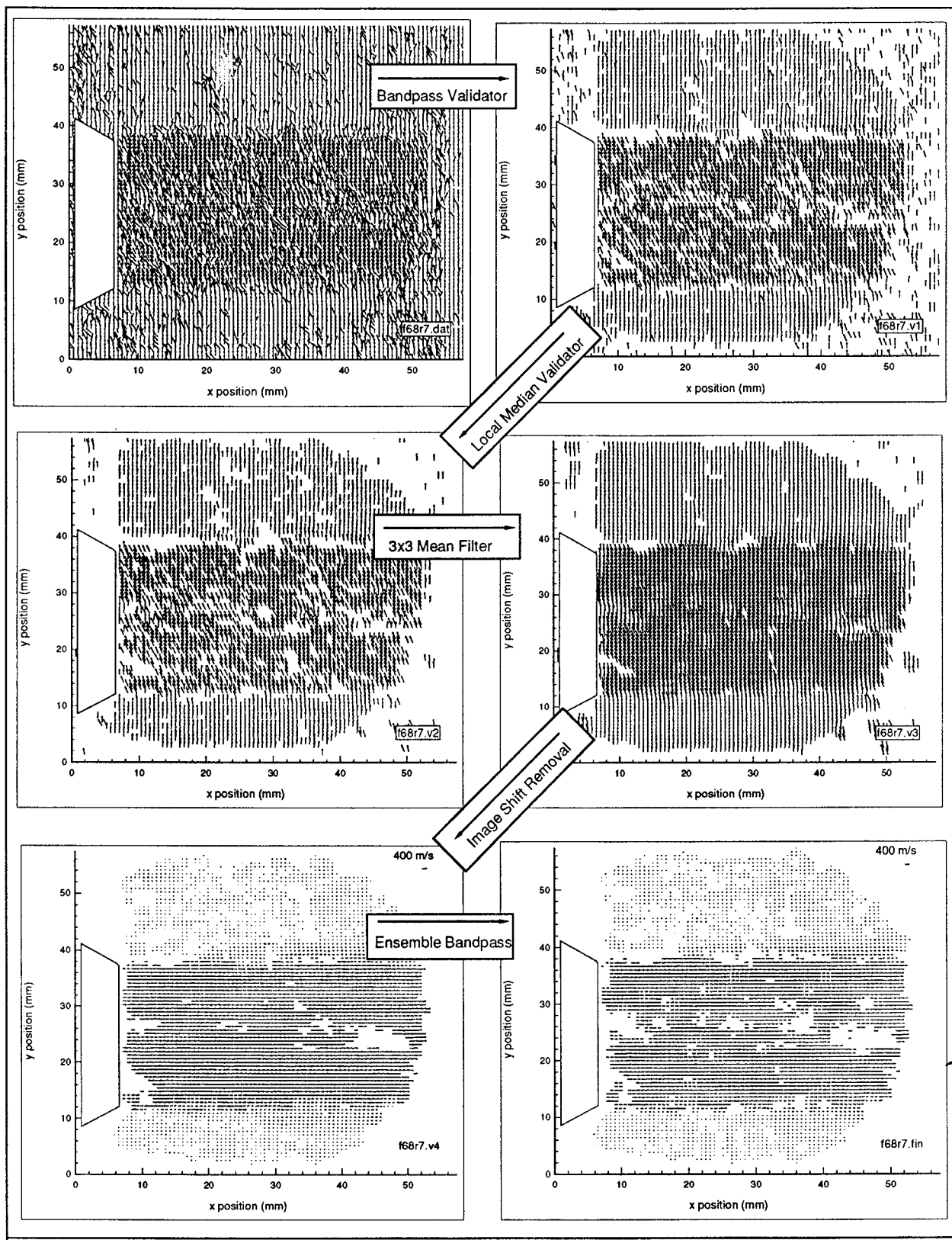
Figure 6. PIV data validation processing steps.
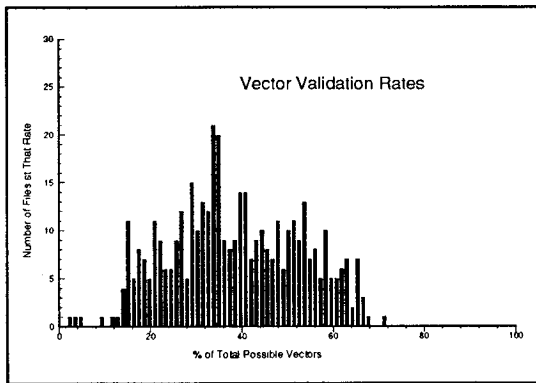
Figure 7. Data vector validation rates.
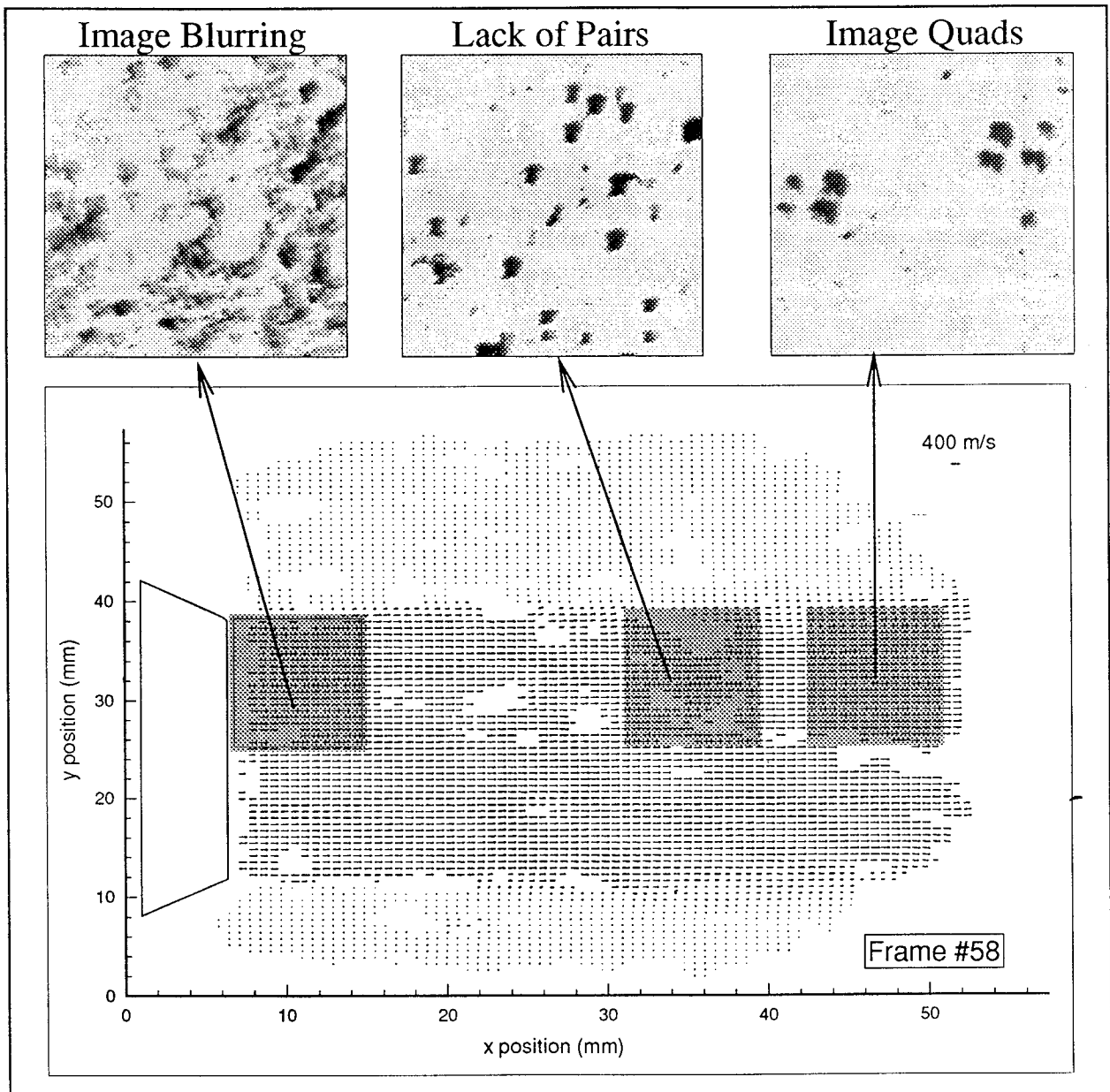
Figure 8. Image quality degradation effects in the flow.

good

quads

blurred

no pairs
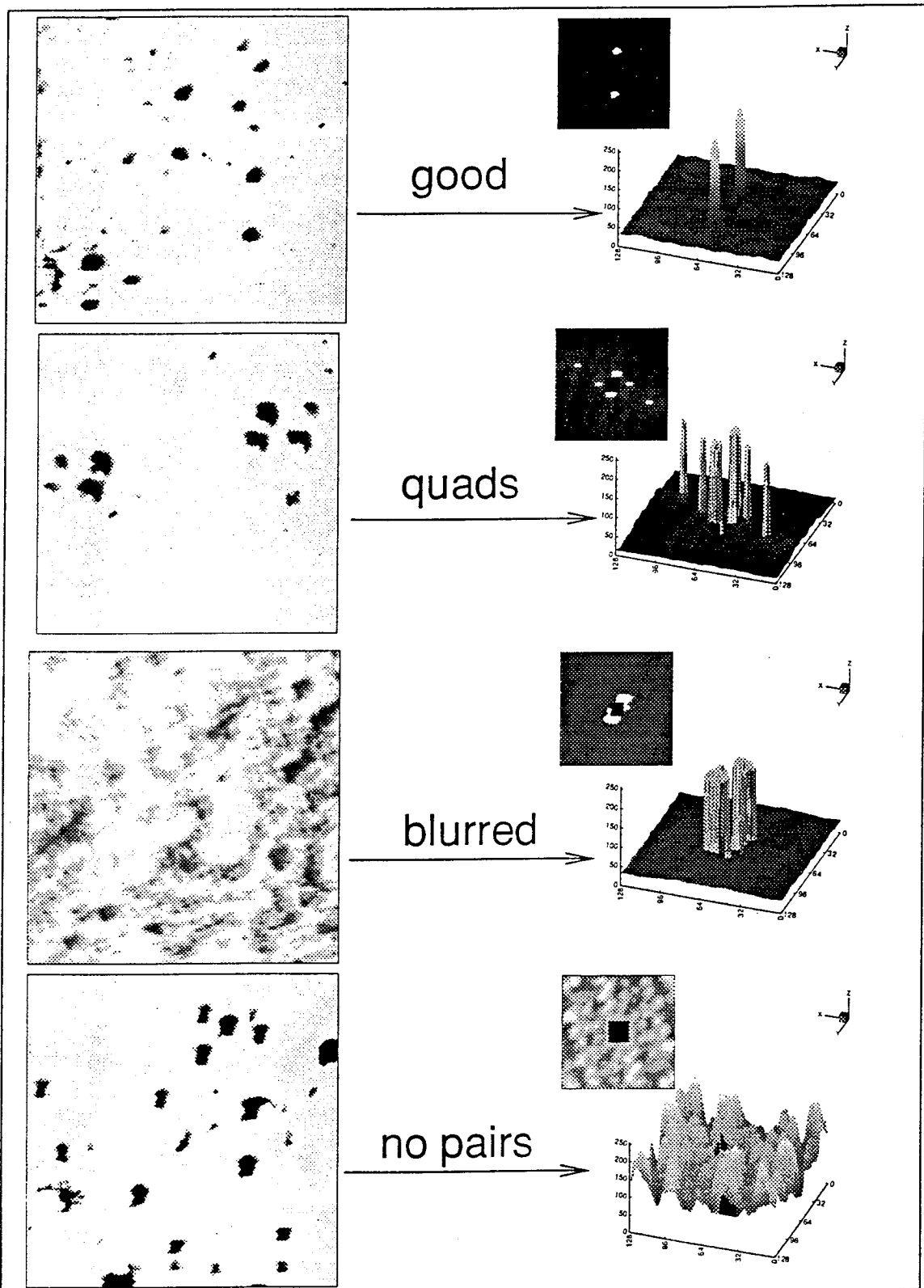
Figure 9. Autocorrelation patterns for various image quality results.
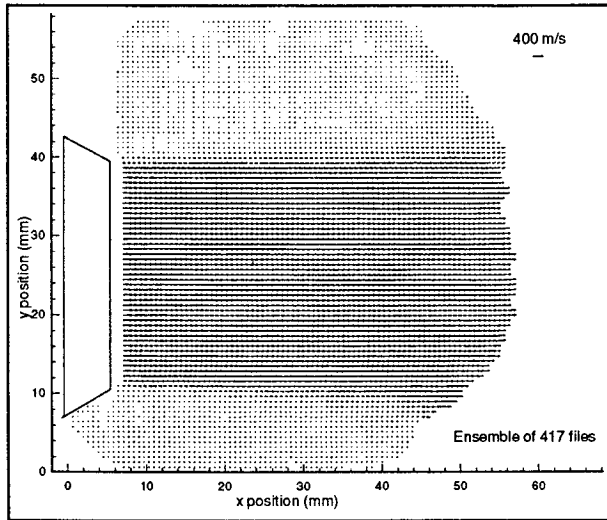
Figure 10. Ensemble mean vector field.
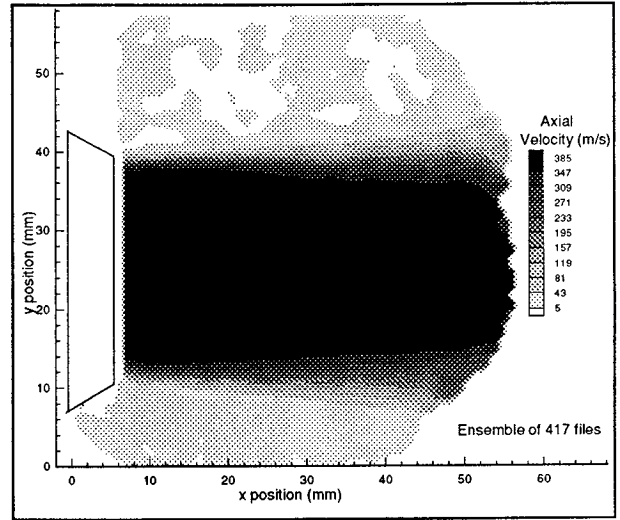
Figure 11. Ensemble mean axial component.
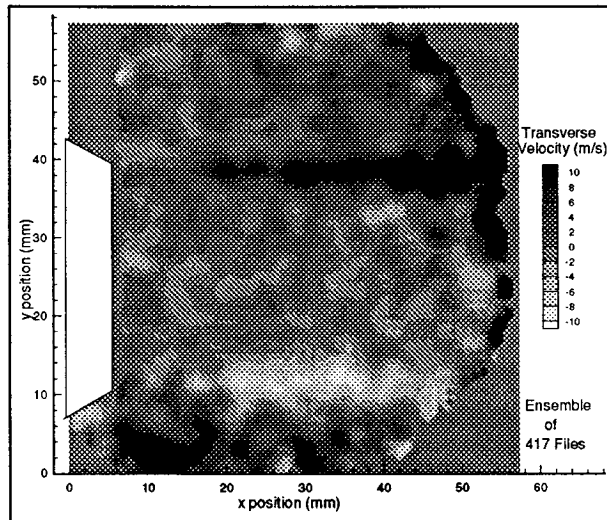
Figure 12. Ensemble transverse component.
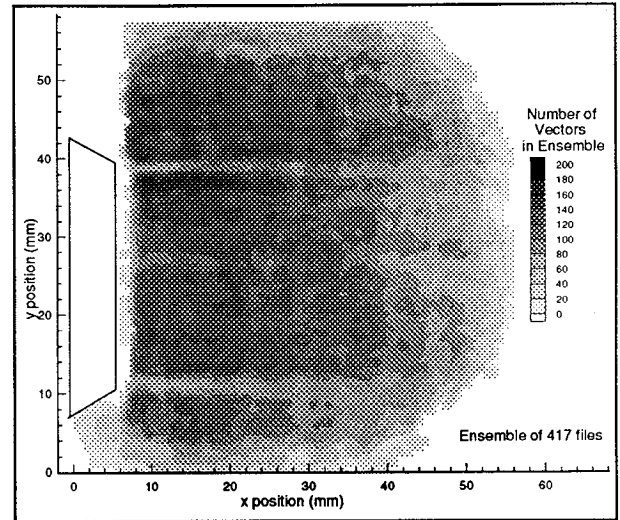
Figure 13. Ensemble number.
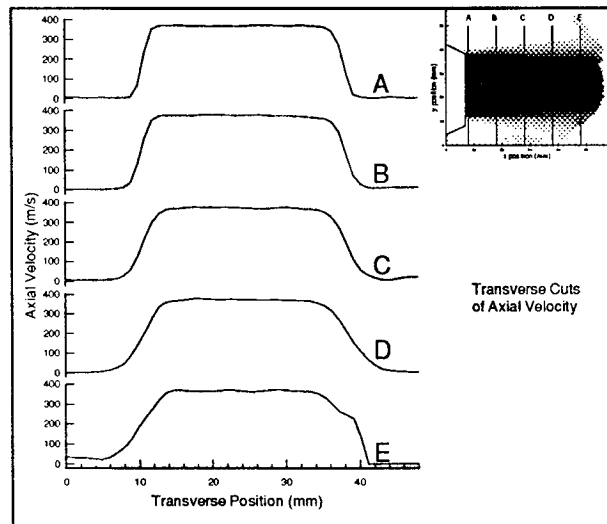
Figure 14. Ensemble mean cross sections.
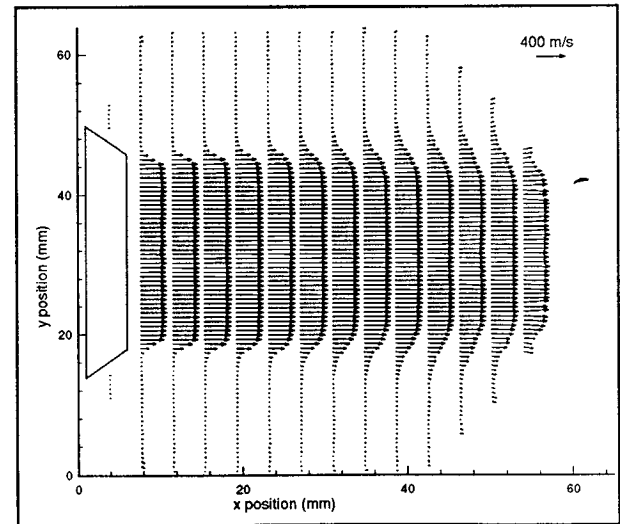
Figure 15. Ensemble mean vector field.

18
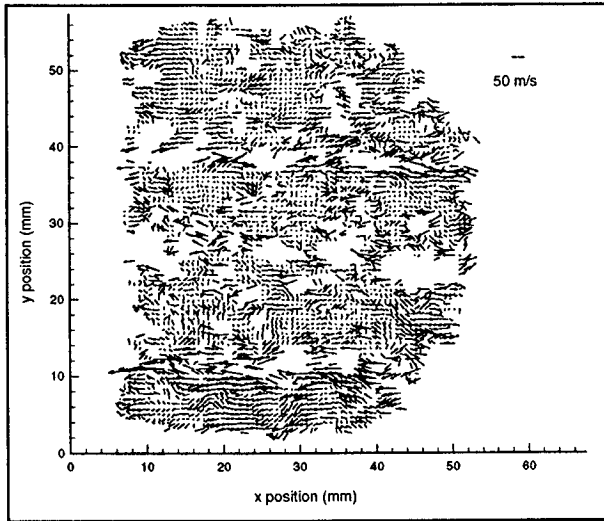
Figure 16. Fluctuating velocity field.
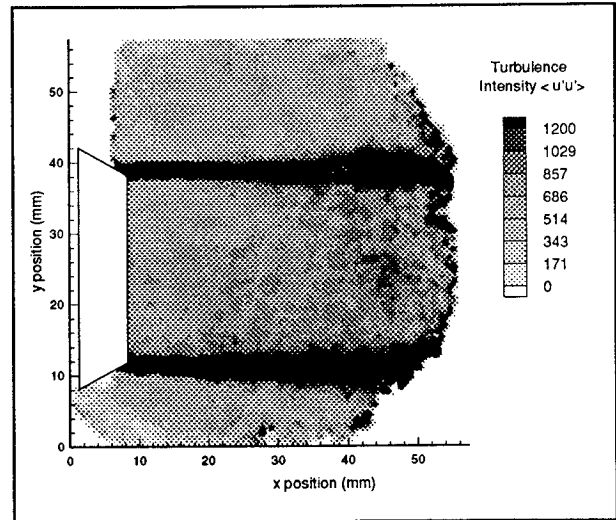
Figure 17. Turbulence intensity <u'u'>.
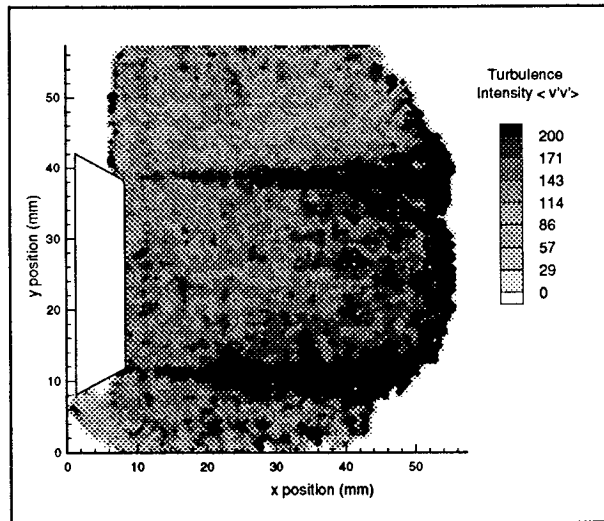
Figure 18. Turbulence intensity <v'v'>.
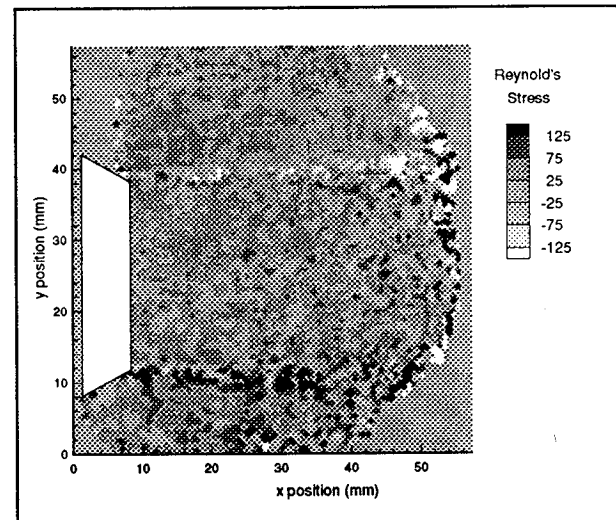
Figure 19. Reynold's Stress <u'v'>.
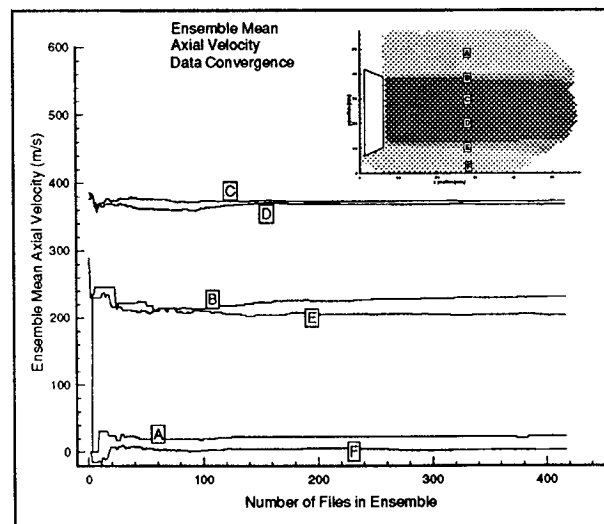
Figure 20. Data convergence of ensemble mean.
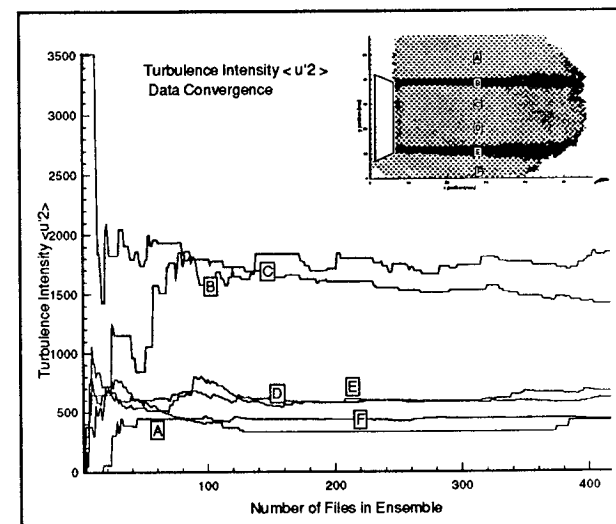
Figure 21. Data convergence of <u'u'>.

19
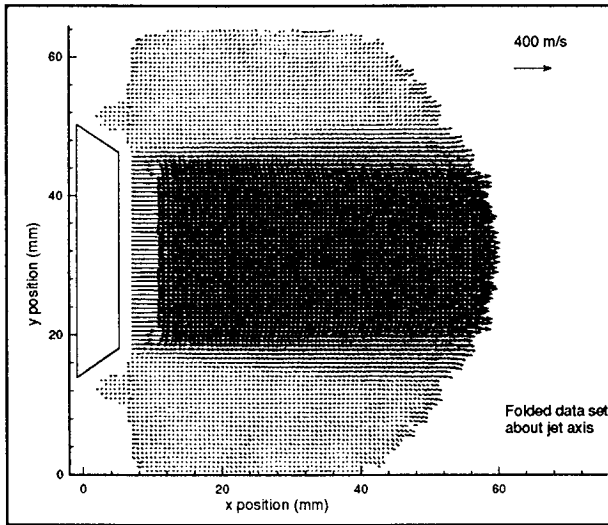
Figure 22. Symmetric folded ensemble mean.
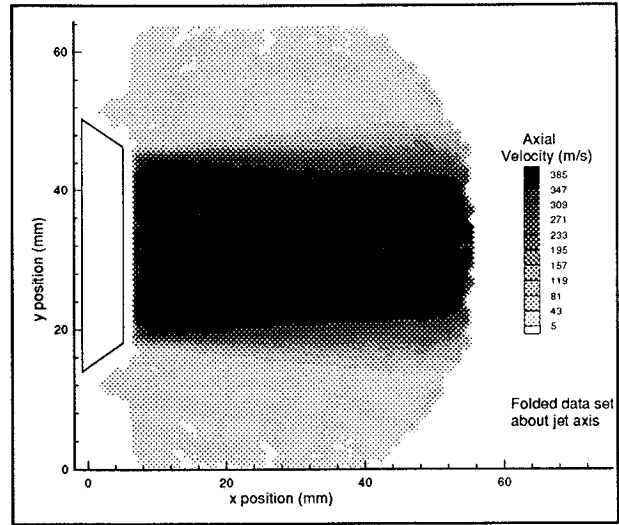
Figure 23. Symmetric folded axial velocity.
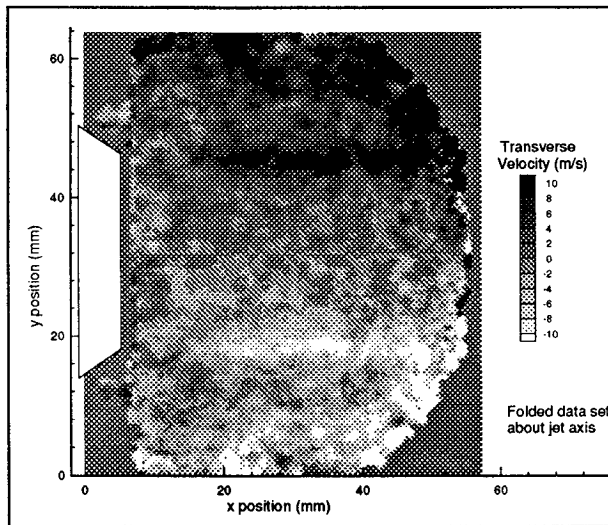
Figure 24. Symmetric folded transverse velocity.
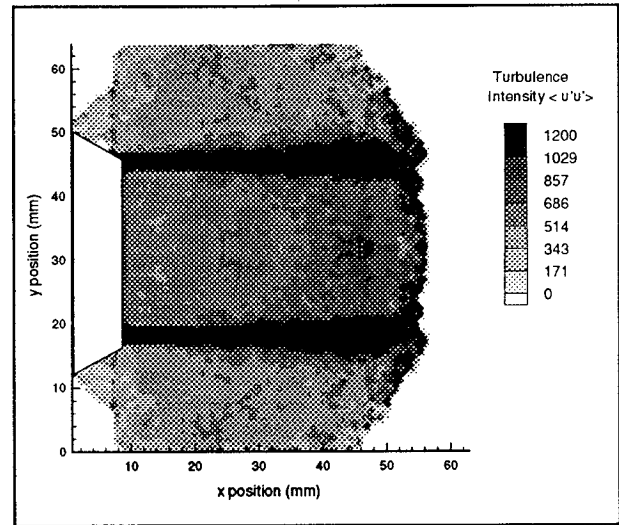
Figure 25. Symmetric folded <u'u'>.
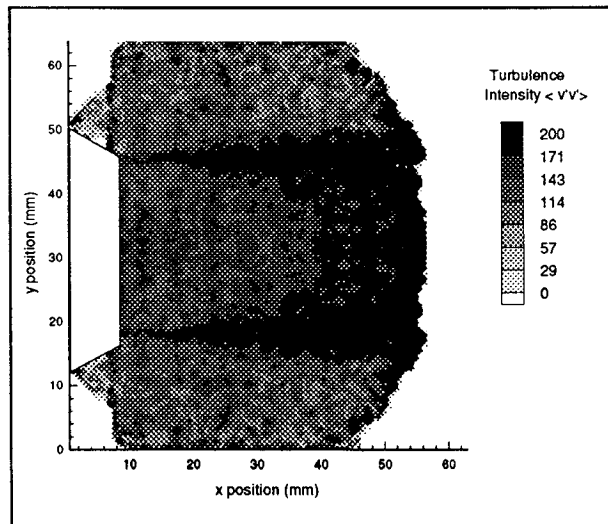
Figure 26. Symmetric folded <v'v'>.
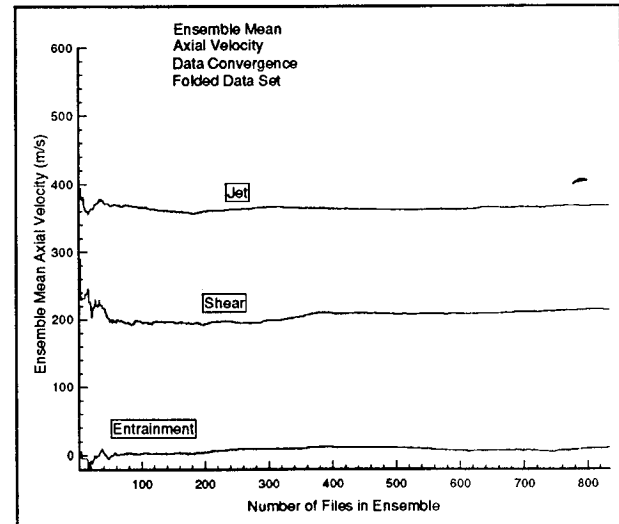
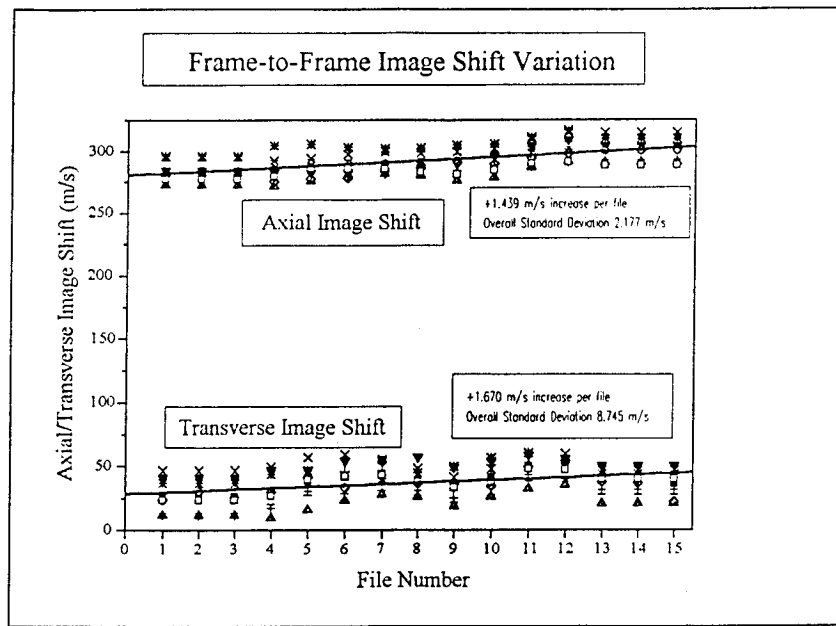Figure 27. Symmetric folded data convergence.
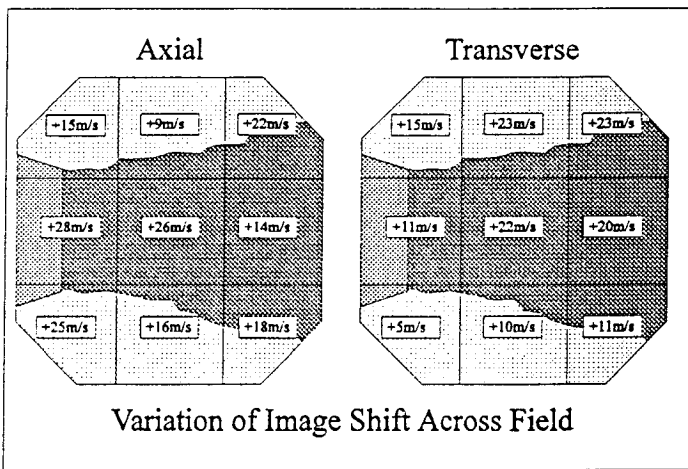
20

Figure 28. Variation of frame-to-frame image shift.

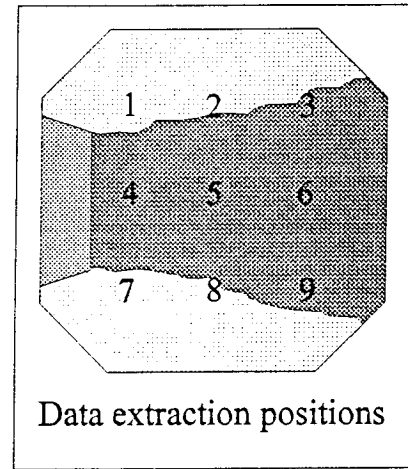Figure 29. Variation of image shift across field of view.

Figure 30. Measurement locations.

| Roll-to-Roll Image Shift Variations							
Film Roll	Mean U (m/s)	Mean V (m/s)	Min/Max U	Min/Max V	ave SDU (m/s)	ave SDV (m/s)	SD Mag (m/s)
Roll 7	23.996	398.195	38.7/12.9	407.6/385.6	6.735	4.011	5.373
Roll 8	-7.272	257.068	-13.9/2.4	265.4/247.7	4.884	4.574	4.729
Roll 9	37.210	291.139	52.4/21.6	304.8/280.8	10.506	8.664	9.585
Roll 11	41.053	400.279	53.2/28.4	407.1/388.3	13.341	9.493	11.417
Roll 15	-39.321	448.112	-53.3/-23.3	459.9/434.0	18.119	8.919	13.519
Roll 16	4.308	344.766	-2.7/23.2	348.7/335.7	6.893	5.665	6.279
Roll 17	-46.874	108.034	-63.1/-35.4	85.6/122.6	15.326	16.135	15.731
Roll 18	-142.734	612.915	-152.2/-134.2	614.1/604.1	25.993	9.058	17.525
Roll 20	56.397	454.381	63.9/48.5	445.2/458.4	18.464	9.259	13.862
Roll 22	-147.581	438.433	-154.9/-134.4	442.3/431.7	14.542	9.349	11.946

Table 1. Variation of image shift across film rolls.
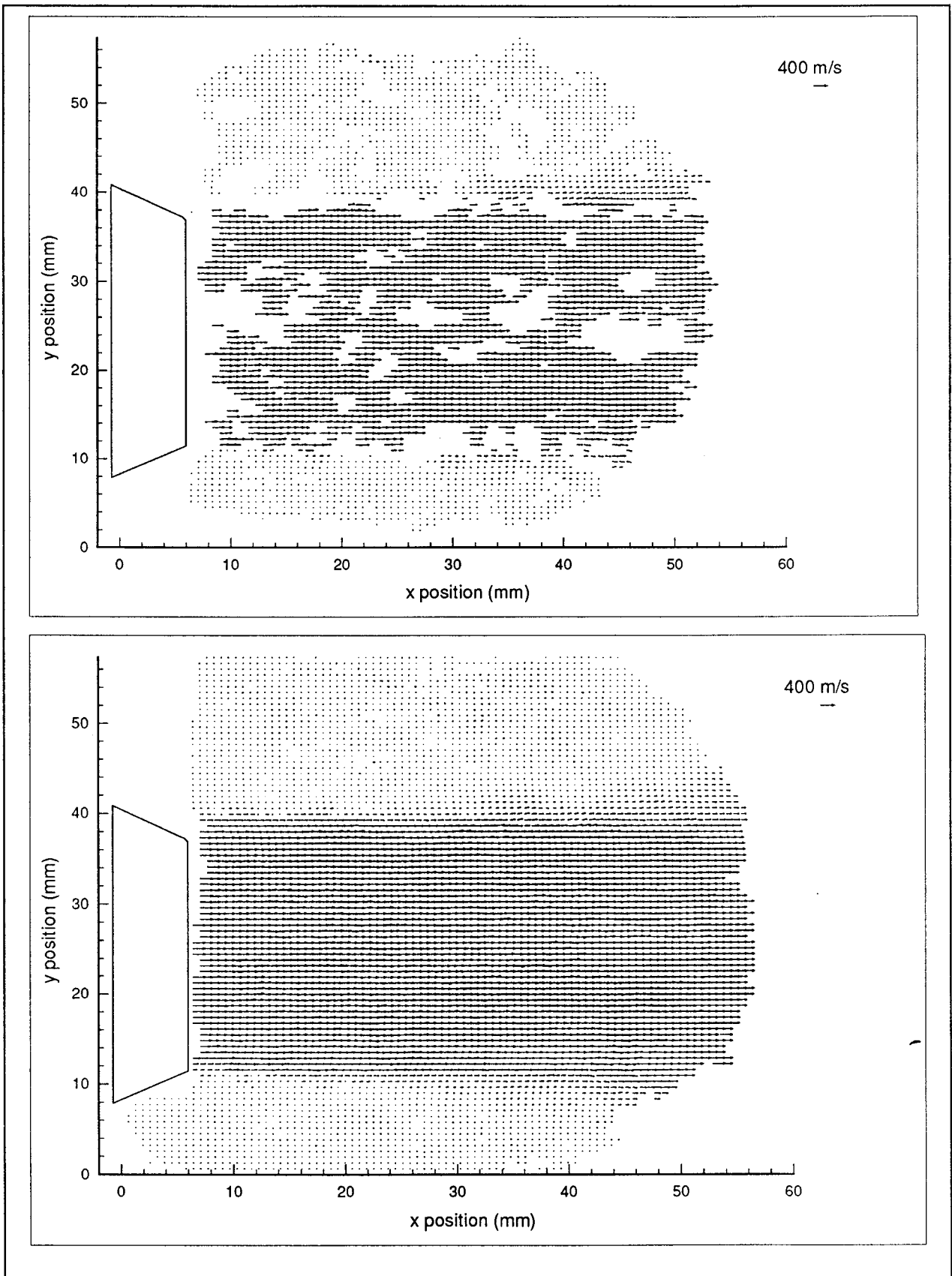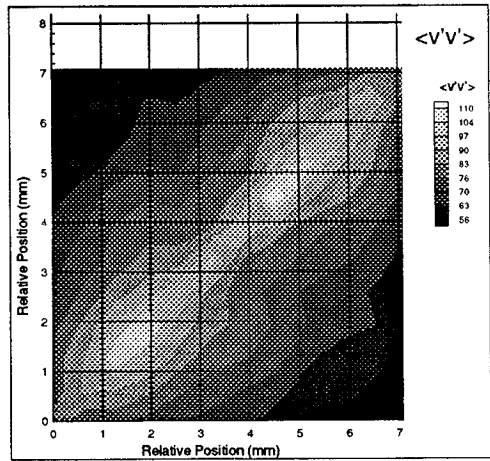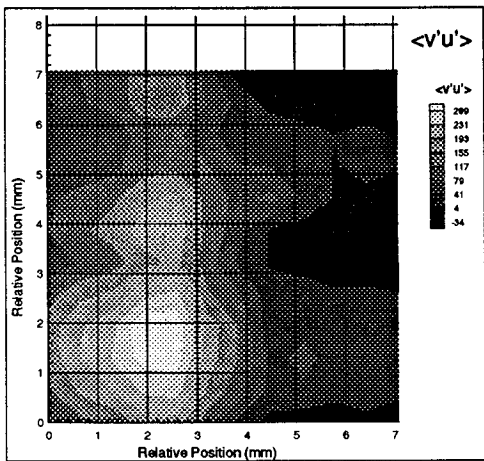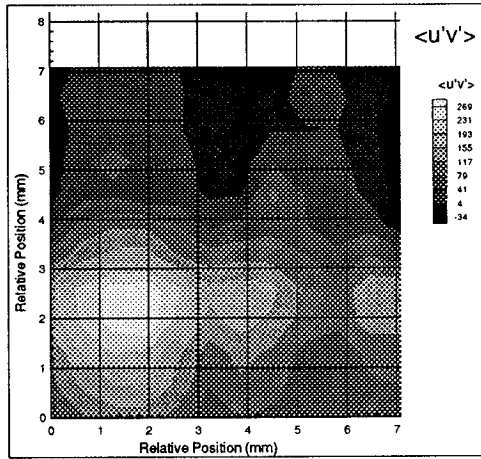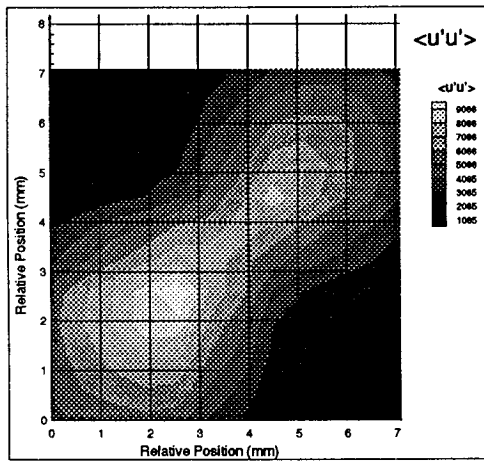
Figure 31. Gaussian interpolator results.

22
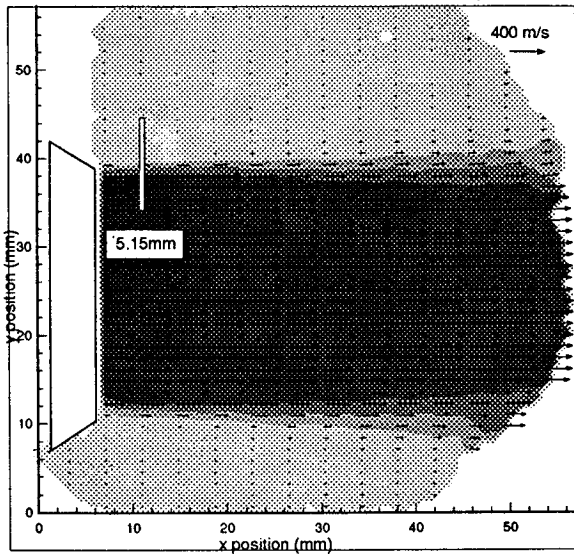
Figure 32. Two-Point correlation results.

REPORT DOCUMENTATION PAGE

Public reporting burden for this collection of information is estimated to average 1 hour per response, including the time for reviewing instructions, searching existing data sources, gathering and maintaining the data needed, and completing and reviewing the collection of information. Send comments regarding this burden estimate or any other aspect of this collection of information, including suggestions for reducing this burden, to Washington Headquarters Services, Directorate for Information Operations and Reports, 1215 Jefferson Davis Highway, Suite 1204, Arlington, VA 22202-4302, and to the Office of Management and Budget, Paperwork Reduction Project (0704-0188), Washington, DC 20503.

1. AGENCY USE ONLY *(Leave blank)*	2. REPORT DATE	3. REPORT TYPE AND DATES COVERED
	January 1997	Contractor Report

4. TITLE AND SUBTITLE

Analysis of Particle Image Velocimetry (PIV) Data
for Application to Subsonic Jet Noise Studies

5. FUNDING NUMBERS

C NAS1 - 19505

WU 538-03-12-04

6. AUTHOR(S)

James L. Blackshire

7. PERFORMING ORGANIZATION NAME(S) AND ADDRESS(ES)

Vigyan, Inc.
30 Research Dr.
Hampton, Va 23666

8. PERFORMING ORGANIZATION REPORT NUMBER

9. SPONSORING/MONITORING AGENCY NAME(S) AND ADDRESS(ES)

National Aeronautics and Space Administration
Langely Research Center
Hampton, Va 23681-0001

10. SPONSORING/MONITORING AGENCY REPORT NUMBER

NASA CR-201665

11. SUPPLEMENTARY NOTES

Langely Technical Monitor : Richard R. Antcliff
Final Report

12a. DISTRIBUTION/AVAILABILITY STATEMENT

Unclassified - Unlimited
Subject Catergory 36

12b. DISTRIBUTION CODE

13. ABSTRACT *(Maximum 200 words)*

Global velocimetry measurements were taken using Particle Image Velocimetry (PIV) in the subsonic flow exiting a 1 inch circular nozzle in an attempt to better understand the turbulence characteristics of its shear layer region. This report presents the results of the PIV analysis and data reduction portions of the test and details the processing that was done. Custom data analysis and data validation algorithms were developed and applied to a data ensemble consisting of over 750 PIV 70 mm photographs taken in the 0.85 mach flow facility. Results are presented detailing spatial characteristics of the flow including ensemble mean and standard deviation, turbulence intensities and Reynold's stress levels, and 2-point spatial correlations.

14. SUBJECT TERMS	15. NUMBER OF PAGES
Particle Image Velocimetry, Jet Noise, 2-point Correlations	24
	16. PRICE CODE A03

17. SECURITY CLASSIFICATION OF REPORT	18. SECURITY CLASSIFICATION OF THIS PAGE	19. SECURITY CLASSIFICATION OF ABSTRACT	20. LIMITATION OF ABSTRACT
Unclassified	Unclassified		

NSN 7540-01-280-5500

Standard Form 298 (Rev. 2-89)
Prescribed by ANSI Std Z39-18
298-102